

**Atmospheric  
inversion for cost  
effective  
quantification of city  
CO<sub>2</sub> emissions**

L. Wu et al.

**Atmospheric inversion for cost effective  
quantification of city CO<sub>2</sub> emissions**

**L. Wu<sup>1</sup>, G. Broquet<sup>1</sup>, P. Ciais<sup>1</sup>, V. Bellassen<sup>2,a</sup>, F. Vogel<sup>1</sup>, F. Chevallier<sup>1</sup>,  
I. Xueref-Remy<sup>1</sup>, and Y. Wang<sup>1</sup>**

<sup>1</sup>Laboratoire des Sciences du Climat et de l'Environnement (LSCE), UMR CEA-CNRS-UVSQ,  
Gif sur Yvette, France

<sup>2</sup>CDC Climat, 75009 Paris, France

<sup>a</sup>now at: INRA, UMR 1041 CESAER, 21000 Dijon, France

Received: 6 August 2015 – Accepted: 3 October 2015 – Published: 5 November 2015

Correspondence to: L. Wu (lwu@lsce.ipsl.fr)

Published by Copernicus Publications on behalf of the European Geosciences Union.

Title Page

Abstract

Introduction

Conclusions

References

Tables

Figures

◀

▶

◀

▶

Back

Close

Full Screen / Esc

Printer-friendly Version

Interactive Discussion

## Abstract

Cities, currently covering only a very small portion (< 3%) of the world's land surface, directly release to the atmosphere about 44 % of global energy-related CO<sub>2</sub>, and are associated with 71–76 % of CO<sub>2</sub> emissions from global final energy use. Although many cities have set voluntary climate plans, their CO<sub>2</sub> emissions are not evaluated by Monitoring, Reporting and Verification (MRV) procedures that play a key role for market- or policy-based mitigation actions. Here we propose a monitoring tool that could support the development of such procedures at the city scale. It is based on an atmospheric inversion method that exploits inventory data and continuous atmospheric CO<sub>2</sub> concentration measurements from a network of stations within and around cities to estimate city CO<sub>2</sub> emissions. We examine the cost-effectiveness and the performance of such a tool. The instruments presently used to measure CO<sub>2</sub> concentrations at research stations are expensive. However, cheaper sensors are currently developed and should be useable for the monitoring of CO<sub>2</sub> emissions from a megacity in the near-term. Our assessment of the inversion method is thus based on the use of several types of hypothetical networks, with a range of numbers of sensors sampling at 25 m a.g.l. The study case for this assessment is the monitoring of the emissions of the Paris metropolitan area (~ 12 million inhabitants and 11.4 TgC emitted in 2010) during the month of January 2011. The performance of the inversion is evaluated in terms of uncertainties in the estimates of total and sectoral CO<sub>2</sub> emissions. These uncertainties are compared to a notional ambitious target to diagnose annual total city emissions with an uncertainty of 5 % (2-sigma). We find that, with 10 stations only, which is the typical size of current pilot networks that are deployed in some cities, the uncertainty for the 1-month total city CO<sub>2</sub> emissions is significantly reduced by the inversion by ~ 42 % but still corresponds to an annual uncertainty that is two times larger than the target of 5 %. By extending the network from 10 to 70 stations, the inversion can meet this requirement. As for major sectoral CO<sub>2</sub> emissions, the uncertainties in the inverted emissions using 70 stations are reduced significantly over that obtained using 10 stations by 32 %

### Atmospheric inversion for cost effective quantification of city CO<sub>2</sub> emissions

L. Wu et al.

Title Page

Abstract

Introduction

Conclusions

References

Tables

Figures

◀

▶

◀

▶

Back

Close

Full Screen / Esc

Printer-friendly Version

Interactive Discussion





erating urbanization process: the global urban population having grown from 746 million in 1950 to 3.9 billion in 2014 while, by 2050, it is expected to grow by 2.5 billion people, with nearly 90 % of them living in Asia and Africa (UN, 2014).

Unlocking the city mitigation potential may significantly reduce the gap of emission reductions between national commitment/pledges and scenarios consistent with a 2 °C limit. A plausible additional city contributions to global emission mitigation was estimated to cover ~ 15 % of the total required global emissions reduction, which represents up to two-thirds of the national commitments/pledges (Erickson and Tempest, 2014). Large urban areas have a strong potential to achieve economies of scale in per capita CO<sub>2</sub> emissions for some important sectors (e.g. transportation and heating) where clusters of population and economic activities can share common infrastructures (Bettencourt et al., 2007; Dodman, 2009; Glaeser and Kahn, 2010; CDP, 2012). Practical city mitigation actions are for instance the improvement of public transportation infrastructure such as Mass and Rapid Transit (MRT) systems, building retrofits and energy/waste recycling, and district heating/cooling plants (Sugar and Kennedy, 2013; Erickson and Tempest, 2014).

Thousands of cities declared to be willing to take actions to report and reduce their CO<sub>2</sub> emissions (Rosenzweig et al., 2010; Reckien et al., 2013). Such efforts can decrease their climate vulnerability and foster co-benefits in terms of air quality, energy access, public health, and city livability (Seto et al., 2014). They also may foster significant local economic development through advances in green technology. For instance, the London low carbon environmental goods and services is estimated to have generated more than GBP 25 billion revenue for 2011/12 (BIS, 2013).

To check whether claimed reduction targets are fulfilled, city emissions will have to be known accurately for present-day conditions to define a baseline upon which reductions are defined, and then monitored over time during any agreed-upon reduction commitment period. Such quantification of emissions and emission reduction echoes the concept of Monitoring, Reporting, and Verification (MRV) that is the cornerstone of most market- or policy-based mechanisms in climate economy (Bellassen and Stephan,

**Atmospheric inversion for cost effective quantification of city CO<sub>2</sub> emissions**

L. Wu et al.

Title Page

Abstract

Introduction

Conclusions

References

Tables

Figures



Back

Close

Full Screen / Esc

Printer-friendly Version

Interactive Discussion



## Atmospheric inversion for cost effective quantification of city CO<sub>2</sub> emissions

L. Wu et al.

Title Page

Abstract

Introduction

Conclusions

References

Tables

Figures

◀

▶

◀

▶

Back

Close

Full Screen / Esc

Printer-friendly Version

Interactive Discussion

2015). The MRV concept integrates three independent processes, namely Measuring or Monitoring (M), Reporting (R), and Verification (V). It ensures that the mitigation actions are properly monitored and reported, and that the mitigation outcomes can be verified. The MRV has been widely applied in many contexts such as projects, organizations, policies, sectors, or activities within territories (see Bellassen and Stephan, 2015, and the references therein). For diverse applications, MRV can rely upon different standards, but requires transparency, quality, and comparability of information about emission accounting and the mitigation action implementations.

The first urban mitigation actions relevant for MRV are those whose impacts are relatively easy to measure, e.g., projects and Programmes of Activities (PoA) under the Clean Development Mechanism (CDM) as well as efforts on emission reductions for large factories and buildings under the Tokyo Emission Trading Scheme (ETS) (Clapp et al., 2010; IGES, 2012; Marr and Wehner, 2012; UNEP, 2014). However, there is a lack of technical capacity for accurate accounting of diffuse sources, e.g. transportation and residential buildings. This lack of capacity makes MRVs for citywide emissions challenging (Wang-Helmreich et al., 2012; UNEP, 2014), and may hinder citywide mitigation implementation in absence of strong political will, sufficient institutional governance and financial support. Hitherto MRV practices for urban mitigation actions are still limited and the majority of sources within the city territory remain uncovered. For instance, the Tokyo ETS – the most advanced urban ETS scheme – only regulates less than 20 % of the city's total emissions (TMG, 2010).

As such, there is a keen need to scale up policy instruments and market mechanisms to foster broader access of supports at various scales from international to local, for enabling citywide mitigation actions (World Bank, 2010; Wang-Helmreich et al., 2012; The Gold Standard, 2014). This gap may be reduced by new mechanisms such as the Nationally Appropriate Mitigation Actions (NAMAs; recent move to raise pre-2020 emission reduction ambitions by increasing access to climate financing) and the New Market-based Mechanism (NMM; currently in negotiation for post-2020 carbon financing about crediting and trading of mitigation outcomes). Both mechanisms are

## Atmospheric inversion for cost effective quantification of city CO<sub>2</sub> emissions

L. Wu et al.

Title Page

Abstract

Introduction

Conclusions

References

Tables

Figures

◀

▶

◀

▶

Back

Close

Full Screen / Esc

Printer-friendly Version

Interactive Discussion



designed under UNFCCC to increase the flexibility of mitigation actions so that broader segments of economy or policy-making can be included in developed and developing countries (Howard, 2014; UNEP, 2014). Based on estimates of emissions from the major sectors, a conceivable approach would be to set up city overall mitigation targets and then negotiate specific targets for individual sectors or groups of sources. Empowered by city-scale MRV (see UNEP (2014) for current developments), city mitigation implementation could be (1) credited or traded under designed mechanisms, and (2) registered for receiving international aide through climate finance. Importantly, all these provisions for citywide mitigation actions and their MRV necessitate the availability of emission accounting methods with required qualities (moderate or stringent; an issue we will discuss in following sections).

The emission accounting methods that are usually suggested are inventories based on statistical data (World Bank, 2010; Wang-Helmreich et al., 2012). Developing city-scale inventories, and updating them over time, involve extensive collection of consistent and comparable emissions data, which measures the level of activities (e.g. energy use statistics, or in a more sector-specific manner, kilometers driven by vehicles, and volume of waste provided to landfill) and the activity-to-carbon conversion rates (i.e. emission factor). In the past, cities have followed diverse guidelines or protocols for emission inventory compilation, and recently there is a trend of centralization e.g. with the newly proposed Global Protocol for Community-Scale Greenhouse Gas Emission Inventories (GPC; Fong et al., 2014) and the UNFCCC reporting platform NAZCA (climateaction.unfccc.int). Admittedly, inventories of city emissions are known to suffer from incomplete and uncertain data (see Appendix A for a brief review of city inventories). For instance, there is usually a lack of precise statistics regarding the total amount of fossil fuel that has been consumed within the cities. This issue of data availability and quality impedes the practical use of city inventories in climate economy.

To improve the quality of emission accounting, here we propose using a new type of data – continuous CO<sub>2</sub> concentration measurements in the atmosphere made on a network of stations around and within cities. Accurate measurements of the atmospheric

signals, e.g. the CO<sub>2</sub> concentration gradients, contain information about the emissions that are independent of inventories. A statistical method known as atmospheric inversion, which has been used for decades for improving the knowledge of global and continental scale natural CO<sub>2</sub> fluxes (Enting, 2002; Bousquet et al., 2000; Gurney et al., 2002; Peters et al., 2007; Chevallier et al., 2010; Broquet et al., 2013), can exploit this information from actual atmospheric measurements for quantifying CO<sub>2</sub> emissions at city scale (McKain et al., 2012; Kort et al., 2013; Lauvaux et al., 2013; Hutyra et al., 2014; Bréon et al., 2015). The principle of an inversion is to combine information from inventory data with atmospheric CO<sub>2</sub> measurements to deliver improved emission estimates, i.e. emissions with a reduced uncertainty, compared to the inventory. An inversion generally uses a 3-D model of atmospheric transport to relate emissions with observations. In just a few years, a number of city atmospheric CO<sub>2</sub> measurement networks have been deployed for pilot studies. Examples of cities where such networks have been deployed are Toronto (with 5 sites), Paris (with 5 sites), Sao-Paulo (with 2 sites), Los Angeles (~ 10 sites), and Indianapolis (with 12 sites). This creates a need to better document the theoretical potential of atmospheric inversions to monitor emissions and their changes or to independently verify inventories, with a quality relevant for city MRV applications.

In this paper, we assess the performance of atmospheric inversions for the monitoring of total and sectoral fossil fuel emissions in the Paris metropolitan area (the Île-de-France (IDF) region, which has ~ 12 million inhabitants). The most resolved regional bottom-up inventory estimates that this area emitted 11.4 TgC in 2010 (AIR-PARIF, 2013), an amount equivalent to ~ 12% of the fossil fuel CO<sub>2</sub> emissions from the whole France (Boden et al., 2013). Urban emissions are mainly connected to emissions from fossil fuel combustion, as other sources of urban emissions such as biofuel uses are usually very limited. Hence, for simplicity, we assume that urban emissions are all from fossil fuel combustion in our study.

In general, there exists no formal agreed-upon minimum requirement about desirable uncertainties in emissions estimates relevant for MRV use. However, such require-

## Atmospheric inversion for cost effective quantification of city CO<sub>2</sub> emissions

L. Wu et al.

Title Page

Abstract

Introduction

Conclusions

References

Tables

Figures

◀

▶

◀

▶

Back

Close

Full Screen / Esc

Printer-friendly Version

Interactive Discussion

---

## Atmospheric inversion for cost effective quantification of city CO<sub>2</sub> emissions

L. Wu et al.

---

Title Page

Abstract

Introduction

Conclusions

References

Tables

Figures

◀

▶

◀

▶

Back

Close

Full Screen / Esc

Printer-friendly Version

Interactive Discussion



ments would give some solid basis to MRV practice for citywide emission mitigation. Therefore, we will first attempt at defining notional targets in terms of uncertainties in the emissions estimates for inversion systems at city scale (Sect. 2.1). In Sect. 2.2, we will then discuss the cost of the observing and modeling systems that are required for atmospheric inversions. This cost, ideally, should be comparable to or even smaller than that of high quality inventories. The observation networks to be tested will be dimensioned to ensure that they fit within this cost. The CO<sub>2</sub> measurement instruments presently used for atmospheric inversion in the scientific community are rather expensive which explains the limited size of the existing city networks. However, cheap sensors are currently developed and we assume here that such sensors will be useable for the inversion of city emissions in the near-term. We will thus assess the performance of the inversion that relies on hypothetical networks similar to the existing ones (limited number of sensors at current cost), or includes a larger number of cheap sensors. The theoretical framework of the inversion allows for the derivation of uncertainty reduction from such hypothetical networks given the statistical description of the sources of error in the inversion configuration. This study is based on the inversion configuration and results using CO<sub>2</sub> measurements from 3 stations in the Paris area, published by Bréon et al. (2015) (hereafter referred to as B15). Taking into account the limited information content from this small network, B15 did not attempt to estimate sectoral emissions separately but rather focused on quantifying total CO<sub>2</sub> emissions from the Paris urban area. The principle of our inversion system extends that of B15 to separate sectoral emissions using larger networks of measurement sites. The use of a large numbers of stations also leads us to conduct network design studies in order to optimize, for a given number of stations, the performance of the inversion as a function of these station locations.

Sections 3 and 4 describe how we use an Observing System Simulation Experiments (OSSE) framework to analyze whether this inversion framework can achieve the uncertainty targets, principally with respect to the number of measurement sensors and their spatial distribution. The inversion methodology and the OSSE setup are described in





toral emission estimates are in general larger than the uncertainties in the aggregated total emission estimate. Due to these reasons, we set notional uncertainty target only for city total emissions estimates in this study.

Succeeding in delivering a 5 % annual uncertainty target for the total emissions of a city would translate into an ability to assess a 25 % reduction of total emissions on a 15-year horizon at 95 % confidence level (detection interval [18, 32 %],  $p = 0.05$  for linear trends of emissions; see Appendix C for numerical details). The Paris climate plan for example, aims at reducing the GHG emission reduction by 25 % by 2020 and by 75 % by 2050 relative to the 2004 baseline (Mairie de Paris, 2012). This means that a 5 % annual uncertainty is also satisfactory to monitor the trend of Paris emissions over time. However, the 5 % target is not a requirement for such trend detection, since, with an annual estimate bearing 10 % uncertainty, a 25 % reduction in 15 years would still remain detectable at 95 % confidence level (detection interval [11, 39 %],  $p = 0.05$ ).

So far, practical atmospheric inversion of the Paris city emissions have been performed over 1-month periods, with an interest in inferring monthly emissions, even though emissions have been actually inverted at a higher temporal resolution (B15). However, our notional target of 5 % uncertainty is defined at the annual scale. One can nevertheless relate monthly uncertainties to annual uncertainty based on one intermediate and two extreme assumptions regarding the temporal correlations between monthly uncertainties: that all monthly uncertainties are independent from one another, that the timescale of these correlations is approximately 2-months, and that all monthly uncertainties are fully correlated. Based on these three assumptions, the annual uncertainty related to the monthly uncertainties can be obtained by simple error propagation. The two extreme cases of null and full positive temporal correlations would hardly happen in reality, but they provide an estimate of the range for such targets. We will consider in control runs a 2-month temporal error correlation of uncertainties in monthly inversion emission estimates in order to derive the most likely corresponding uncertainty in the annual inversion estimates. For instance, a 20 % 1-sigma monthly uncertainty corresponds to 12, 23, 40 % 2-sigma annual emission uncertainties, given

**Atmospheric inversion for cost effective quantification of city CO<sub>2</sub> emissions**

L. Wu et al.

Title Page

Abstract

Introduction

Conclusions

References

Tables

Figures



Back

Close

Full Screen / Esc

Printer-friendly Version

Interactive Discussion





## Atmospheric inversion for cost effective quantification of city CO<sub>2</sub> emissions

L. Wu et al.

Title Page

Abstract

Introduction

Conclusions

References

Tables

Figures

◀

▶

◀

▶

Back

Close

Full Screen / Esc

Printer-friendly Version

Interactive Discussion

The cost of an inventory involves mainly data collection, and the design and implementation of the inventory methodology. The data (e.g. statistics on energy fuel consumption, transport and industrial activities) required for the development of a national inventory are in general available from national agencies, and the cost of its collection is on the order of several million euros per country per year (Chang and Bellassen, 2015). However, most of the cost incurs from collecting socio-economic data that are primarily obtained for other political/economical/social purposes than emission inventory. The CITEPA is the agency responsible for preparing the French national inventory along the IPCC guidelines. The budget of the activities at CITEPA related to this inventory is on the order of 1 MEUR year<sup>-1</sup> (PLF, 2014). This cost covers the compilation of the fossil fuel CO<sub>2</sub> emissions inventory but also (1) the compilation of the inventory for other GHG gases, (2) the compilation of the inventory for GHG emissions due to land use, land use change and forestry (LULUCF), and (3) activities other than monitoring such as the reporting, archiving and annual communication to UNFCCC reviews that are imposed by the IPCC guidelines. It is therefore complicated to assess the part of the cost that is dedicated to the compilation of the CO<sub>2</sub> fossil fuel emissions inventory by CITEPA. As for the city inventory compilation, tracking fuel use statistics from different origins and types and for different sectors might in fact prove more complicated than for a state where national statistics are already firmly established by governmental agencies. As a result of the above discussions, we will assume in this study that building and updating each year a city inventory for the Paris metropolitan area that could possibly achieve the 5% notional annual uncertainty target would cost around 0.5 MEUR year<sup>-1</sup>.

The cost of the observation network for atmospheric inversion is related to that of the measurement instruments and to that of the calibration and maintenance procedures that ensure limited drift and biases in the measurements. We consider two types of sensors that could equip the city observation networks: “high precision sensors” (e.g. existing cavity ring down spectrometers employed by current research networks) and “cheap sensors” currently still in development but likely available in the near future

## Atmospheric inversion for cost effective quantification of city CO<sub>2</sub> emissions

L. Wu et al.

Title Page

Abstract

Introduction

Conclusions

References

Tables

Figures

◀

▶

◀

▶

Back

Close

Full Screen / Esc

Printer-friendly Version

Interactive Discussion



(see Appendix B for details). High precision sensors are instruments with a precision of 0.1 ppm (1-sigma) on hourly measurements. Given the present calibration procedures, such hourly measurements bear additional systematic errors that are smaller than 0.13 ppm for hourly measurements. “Cheap sensors” are expected to have lower precision. The threshold for such precision will be defined in this study to be 1 ppm on hourly measurements, and the precision target will be actually 0.5 ppm (1-sigma). We also hypothesize that calibration procedures for the cheap sensors, with costs that are comparable to that for high precision sensors, should ensure that the systematic error in hourly measurements is smaller than 1 ppm. Given that the systematic errors should not have long autocorrelation timescales and that precision errors are not autocorrelated in time (see Appendix B), these different errors for both the high precision instruments and the cheap sensors should be far smaller than the errors associated with atmospheric transport modeling and they are thus ignored hereafter (see Sect. 3.5.2 for details). Hence, in this study, the only impact of using one or the other type of sensor is thus related to their cost. Given the consideration regarding the limitation of the cost of the atmospheric inversion, this leads to different numbers of stations allowed for the network of measurement sites. With the notional budget of 0.5 MEUR year<sup>-1</sup>, one could afford to operate a network of either ~ 10 high precision sensors or ~ 70 cheap sensors (see Appendix B). We thus evaluate the performance of the inversion in terms of uncertainty reduction when using hypothetical measuring networks of 10 to 70 sensors.

### 3 Methodology

#### 3.1 Bayesian inversion

By Bayesian inversion, the information from an observation vector  $\mathbf{y}$  is combined with a prior (background) estimate  $\mathbf{x}^b$  of a control parameter vector  $\mathbf{x}$  about CO<sub>2</sub> emissions

to provide an updated estimate  $x^a$  (Enting, 2002):

$$x^a = x^b + \mathbf{B}\mathbf{H}^T(\mathbf{R} + \mathbf{H}\mathbf{B}\mathbf{H}^T)^{-1}(\mathbf{y} - \mathbf{H}\mathbf{x}^b), \quad (1)$$

where  $\mathbf{H}$  the linear matrix operator linking  $\mathbf{y}$  with  $\mathbf{x}$  based on the modeling of emissions and atmospheric transport. The errors in  $\mathbf{y}$ ,  $\mathbf{H}$  and  $\mathbf{x}^b$  are assumed to have statistical distributions that are Gaussian, unbiased and independent of one another. We denote by  $\mathbf{R}$  and  $\mathbf{B}$  the covariance matrices of the observation and background errors respectively. The observation error is a sum of measurement and model errors. Similar to B15, we control a vector  $\mathbf{x}$  of the budgets of emission estimates, which all together constitute the total emissions of IDF for the month of January 2011. These emissions are defined on a spatial horizontal grid same as that of the atmospheric transport model (see Sect. 3.4.2 for the definition of this grid covering IDF). Here, the observation operator  $\mathbf{H}$  can be decomposed into a chain of three operators: the spatial and temporal distribution of the budgets of emissions within a corresponding area and period of control, the atmospheric transport of  $\text{CO}_2$  given these spatial and temporal distributions of the emissions, and a sampling of the resulting simulated  $\text{CO}_2$  to be compared with the observations (Fig. 1). These three  $\mathbf{H}$  components will be detailed later in Sect. 3.4. According to the theory of Best Linear Unbiased Estimation (BLUE), the inversion system (Eq. 1) provides an emission estimate  $x^a$  with reduced uncertainty (i.e. with “smaller” error covariance matrix compared to  $\mathbf{B}$ ):

$$\mathbf{A} = (\mathbf{B}^{-1} + \mathbf{H}^T\mathbf{R}^{-1}\mathbf{H})^{-1}. \quad (2)$$

Here we assess the inversion performance by evaluating the ability of inversion to reduce uncertainties in emission estimates, which can be computed by Eq. (2) using realistic prior and observation error statistics. This assessment is done for the estimation of the emissions during the month of January 2011. In the following sections, we detail each component of the inversion system for this computation (see Fig. 1).

Atmospheric  
inversion for cost  
effective  
quantification of city  
 $\text{CO}_2$  emissions

L. Wu et al.

Title Page

Abstract

Introduction

Conclusions

References

Tables

Figures

◀

▶

◀

▶

Back

Close

Full Screen / Esc

Printer-friendly Version

Interactive Discussion



## 3.2 Control vector

Formally, even though this is equivalent in principle,  $\mathbf{x}$  does not directly contain emission budgets, but scaling factors that are applied to emission budgets included in the observation operator  $\mathbf{H}$ . Each scaling factor in the control vector  $\mathbf{x}$  corresponds to the budget of emissions for a given spatial area of the IDF domain, a given temporal window, and a given sector or group of sectors of CO<sub>2</sub> emitting activity. The corresponding ensemble of areas, temporal windows and sectors form partitions of the IDF domain, of the month of January and of the full range of emitting activities respectively, so that the different control variables are associated with a partitioning of the total emissions in IDF during January 2011. Hereafter, we will call a “control tile” the combination of an area, a temporal window and a sector (or group of sectors) associated with a control variable. While it is desirable to solve for the emissions at high spatial, temporal and sectoral resolution (in order to avoid aggregation errors, see below), the size of the control vector, and thus this partitioning, must be limited due to computational constraint for inversions. In practice, the partitioning described below is adapted to the sectorial, temporal and spatial distribution of the emissions (using insights from the inventory presented in Sect. 3.4.1). We did not estimate the emissions outside of the IDF region.

We group the various sectors usually provided by inventories (detailed in Sect. 3.4.1) according to the New Format Reporting (NFR) nomenclature defined by the Long-range Transboundary Air Pollution (LRTAP) Reporting Guidelines (EEA, 2013) into seven groups of sectors (see Appendix A for details), namely (1) surface commercial and residential building heating/cooling, (2) road transport, (3) energy production (power plants), (4) combustion and production processes in industries, (5) combustions from agricultural activities, (6) airline traffic, and (7) the rest of all other sectors with smaller emission budgets (e.g. railway, navigation, fugitive emissions, and several minor production processes). These seven sectors are labeled for short as building, road, energy, production, agriculture, airline, and rest, respectively.

### Atmospheric inversion for cost effective quantification of city CO<sub>2</sub> emissions

L. Wu et al.

Title Page

Abstract

Introduction

Conclusions

References

Tables

Figures



Back

Close

Full Screen / Esc

Printer-friendly Version

Interactive Discussion



---

## Atmospheric inversion for cost effective quantification of city CO<sub>2</sub> emissions

L. Wu et al.

---

Title Page

Abstract

Introduction

Conclusions

References

Tables

Figures

◀

▶

◀

▶

Back

Close

Full Screen / Esc

Printer-friendly Version

Interactive Discussion

In order to save computations, for most of these sectors (isolated energy and production point sources, agriculture, airline and rest), we consider that the spatial area of control for the inversion is the whole IDF area. However, for the two important building and road emissions, we spatially partition IDF into five zones for which the fluxes will be optimized: a central zone (approximately the administrative definition of the city of Paris, which is very densely populated) and four surrounding areas (the north-west, south-west, north-east and south-east areas of the remaining IDF region, with borders adapted to the distribution of the building and road emissions, see Fig. 2).

Regarding the temporal partitioning, for the three sectors which have the smallest budgets of emissions (agriculture, airline, and rest), the temporal resolution of the control vector is daily. For the four other sectors (building, road, energy and production), we refine the temporal resolution to control separately the daytime (09:00–18:00 LT) and night-time (18:00–09:00 LT) emissions for each day, in order to account for the large diurnal variations in the emissions.

Atmospheric CO<sub>2</sub> observations are sensitive to vegetation-atmosphere CO<sub>2</sub> fluxes in addition to fossil fuel CO<sub>2</sub> emissions. For cities surrounded by vegetation or containing green areas, the impact of vegetation-atmosphere CO<sub>2</sub> fluxes on city carbon balance can be significant. For instance, Nordbo et al. (2012) estimated that a city is carbon-neutral when its green-area fraction is about 80 %. However the impact of natural vegetation on our results for the highly urbanized IDF region is found limited (see the Supplement). In our inversion, we account for the influence of NEE by including, in the control vector, the scaling factors for the budgets of NEE in the full modeling domain (see Sect. 3.4) and for the four different 6 h windows of the day (i.e. 00:00–06:00, 06:00–12:00, 12:00–18:00, and 18:00–24:00 h LT) over different 5-day periods during January 2011. The number of NEE scaling factors included in the control vector is thus 24, and the total number of scaling factors is 834 (see Table 1 for details).

### 3.3 Observations

We use an inversion system similar to that of B15, in which observations are taken to be CO<sub>2</sub> atmospheric concentration gradients between city upwind and downwind stations. B15 also suggested assimilating only afternoon gradients when the wind speed is above a given threshold. By selecting afternoon gradients, we avoid biases in the vertical mixing during nighttime, mornings and evenings when mesoscale transport models have difficulties in representing the planetary boundary layer (Seibert et al., 2000; Steeneveld et al., 2008). Selecting data for high wind speed limits the signature in the atmospheric measurements of local sources that are in the vicinity of the measurement sites and that cannot be represented correctly by the transport model.

For investigating the potential of the inversion as a function of the observation network, we consider three strategies to deploy a given number of stations. These strategies define three corresponding types of networks: the Elliptical (E), Uniform (U) and Random-even (R) networks (Fig. 3). The E networks surround emissions in the city center, and appear suitable to the assimilation of city upwind-downwind gradients. The E networks consist in three concentric ellipses or rings of stations around the main part of the Paris urban area (the Paris administrative city and its 3 surrounding administrative circumscriptions), encompassing almost all the urban area of IDF. The U networks are defined by a positioning of the stations on a regular grid. The R networks aim at balancing the positioning of stations near the city center and in the surrounding areas. The R networks have thus denser coverage over the city center and fewer stations in the surrounding zones than the U networks, but they still cover the whole IDF domain. Apart from the E networks, the U and R networks have stations both close to the emissions in the Paris urban area and in rural areas in its vicinity.

We assess the potential of the inversion when using these networks with either 10, 30, 50, or 70 stations. For a given network, the station locations are chosen as a subset of a predefined set of 90 candidate locations, depending on the type of the network. For example, 14, 24 and 52 of the 90 candidate stations for R networks are located in

## Atmospheric inversion for cost effective quantification of city CO<sub>2</sub> emissions

L. Wu et al.

Title Page

Abstract

Introduction

Conclusions

References

Tables

Figures

◀

▶

◀

▶

Back

Close

Full Screen / Esc

Printer-friendly Version

Interactive Discussion











---

**Atmospheric  
inversion for cost  
effective  
quantification of city  
CO<sub>2</sub> emissions**L. Wu et al.

---

[Title Page](#)[Abstract](#)[Introduction](#)[Conclusions](#)[References](#)[Tables](#)[Figures](#)[◀](#)[▶](#)[◀](#)[▶](#)[Back](#)[Close](#)[Full Screen / Esc](#)[Printer-friendly Version](#)[Interactive Discussion](#)

downwind station (read from the ECMWF meteorological product). We impose that the direction angle between the upwind and downwind stations should be comprised between  $\pm 11.25^\circ$  of the wind direction at the downwind station (defining a  $22.5^\circ$  angle of selection). Figure 5 shows the wind direction for a downwind observation and the area that covers its corresponding upwind candidate stations. Then we further impose that the distance between the upwind and downwind stations should be larger than 5 km and as close as possible to 10 km. This distance would correspond to the advection of an air parcel during 1 h with a wind speed of  $3 \text{ ms}^{-1}$  (i.e. our threshold on the wind speed for the assimilation of gradients). Here, we ignore the time lag needed to advect an air parcel from upwind to downwind stations and compute gradients between simultaneous hourly mean observations. We discard the observations for which no upwind station can be found based on our selection rules. About 7–16% of observations are retained for gradient computation with this data selection procedure, depending on the size and type of the networks.

Figure 6a shows the afternoon hourly wind conditions at an example station called EVE26 during January 2011, and Fig. 6b shows the wind directions corresponding to the selection of upwind stations when EVE26 is downwind. Winds over station EVE26 blow prevalingly along the southwest-northeast direction for this period (Fig. 6a). Since EVE26 is located to the northeast of the urban center (Fig. 6c), upwind stations for gradient computation are mostly selected in the southwest direction (Fig. 6b and c).

Eight CHIMERE simulations with, in input, respectively the simulation of the NEE in Northern France and the inventories for the 7 sectors of the fossil fuel emissions in IDF described in Sect. 3.4.1 are used to check the contributions of each flux component to the CO<sub>2</sub> mixing ratio variations at network stations. This corresponds to applying **H** to control vectors with scaling factors corresponding to the NEE or to a specific sector of emission set to 1 and others to 0, ignoring CO<sub>2</sub> boundary conditions. Figure 7 plots the resulting CO<sub>2</sub> mole fractions at 10 stations of an R network (which are indicated by red triangles in Fig. 5) including 2 urban stations (EVE07 and EVE11 in Fig. 6c) and 8 rural stations.







## Atmospheric inversion for cost effective quantification of city CO<sub>2</sub> emissions

L. Wu et al.

Title Page

Abstract

Introduction

Conclusions

References

Tables

Figures

◀

▶

◀

▶

Back

Close

Full Screen / Esc

Printer-friendly Version

Interactive Discussion



the fluxes outside the IDF area, whose cancelling is the main aim of the gradient computation. Even though their system potentially bears higher aggregation errors since using a coarser control vector, this should not be highly significant and we derive the estimate of the model errors for our study based on their diagnostics and on a simple derivation of the spatial correlations of the model error between the stations that can lead to their results. This leads us to assign a standard deviation of 3.5, 5.6, and 7 ppm respectively for the observation error on gradients between rural stations, between rural and urban stations and between urban stations. Alternative settings such as inflated (50 % larger) or shrunk (50 % smaller) standard deviation of the observation errors lead to insignificant changes in inversion results (see Supplement Fig. S1).

## 4 Results

We conduct inversions of sectoral and total emissions during the month of January 2011 using E, R and U networks with 10, 30, 50 and 70 stations. The inversion results are analyzed in terms of posterior uncertainties in the inverted fluxes and in terms of uncertainty reduction by the inversion (Fig. 8). The uncertainties discussed here are relative uncertainties, which are defined as the uncertainty budgets in percentage to the budgets of the corresponding prior emissions obtained from the IER inventory.

We find that, with small E, R or U networks of 10 stations (i.e. the size of some of the existing networks), inversions are effective in reducing uncertainties in total emissions as well as in the emissions from the three major sectors (building, road and energy). The inversion reduces on average the 1-sigma uncertainty in the total emissions estimates from  $\sim 19\%$  a priori down to  $\sim 11\%$  a posteriori (a 42 % uncertainty reduction). This posterior uncertainty would correspond to a 13 % 2-sigma uncertainty in annual inverted emissions if assuming approximately 2-months temporal correlation between monthly uncertainties (see Sect. 2.1). This level of posterior uncertainty does not meet the notional target of 5 % 2-sigma annual uncertainty. The 1-sigma uncertain-

## Atmospheric inversion for cost effective quantification of city CO<sub>2</sub> emissions

L. Wu et al.

Title Page

Abstract

Introduction

Conclusions

References

Tables

Figures

◀

▶

◀

▶

Back

Close

Full Screen / Esc

Printer-friendly Version

Interactive Discussion

ties in building, road and energy emission estimates for the month of January 2011 are reduced on average from  $\sim 36\%$  (prior uncertainty) down to about 23, 27 and 24 % respectively. Even though it represents high uncertainty reductions (about 35, 23 and 31 % of gain respectively over the prior uncertainty), these levels of posterior uncertainties are above the threshold of level 1 quality that has been defined in Sect. 2.1. In contrast, the uncertainty reduction is very limited for emissions from agriculture, airline, production, and rest sectors. However, the contribution of these four sectors of emissions to the total budget is rather small, which represents only  $\sim 16\%$  of the total emissions in IDF according to the IER inventory (Fig. 8e). Note that, in order to limit the influence of specific station locations, we performed inversions with 10 random networks of the same type and size. These random networks differ from one another in their station locations, but still keep the feature of the type of network (see Sect. 3.3 on how we generated these random networks). The variation (error bars in Fig. 8) in inversion performance due to the influence of station locations is in general small, compared to the variations influenced by the network type and size (see Fig. 8). This influence of station locations for the agriculture sector is significant, but the budget of agriculture emissions is very small.

The gain in uncertainty reduction by inversions increases with larger networks. However, this increase slows down and is rather weak once the networks have more than 30 stations (Fig. 8a–c). While there is not much difference between the uncertainty reduction for energy emission estimates when using 30-station or 70-station E networks (Fig. 8a), the increase in uncertainty reduction for building emissions when using 30-station or 70-station U networks is still significant. To further illustrate this saturation effect, we assess the number of Degrees of Freedom for the Signal (DFS) of the different networks (Fig. 10a). The DFS describes how many degrees of freedoms of measurements are related to the signal. The simplest illustrating case is that a measurement  $y$  estimates an emission  $x$  with an error  $\epsilon$ :  $y = x + \epsilon$ , where the prior and measurement errors are independent of each other with variances being  $v^b$  and  $v^\epsilon$  respectively. The measurement  $y$  will provide one degree of freedom about  $x$  if there is



20% respectively. Large networks are more promising for the estimation of dispersed surface emissions such as that from the building sector.

An important finding of our study is that different types of networks show distinct ability for monitoring emissions, which is usually sector-specific. For instance, using a U instead of a E 70-station network leads to 18 vs. 22%, 18 vs. 19%, 15 (i.e. a level 2 quality) vs. 18%, and 6 (i.e. a level 3 quality) vs. 9% (i.e. a level 2 quality) differences in the posterior uncertainty in the estimates of the energy, road, building and total emissions (Fig. 8d). Therefore, with 70-station U networks, the target of 5% 2-sigma annual uncertainty for the total emission estimate can be met. Compared to the U networks, the E networks result in larger DFS values (Fig. 10a) but worse performances in uncertainty reduction for total emission estimates (Fig. 10b). The stations in the E network are around the area of high emissions (in particular central Paris), therefore their concentration gradients would be overall more sensitive to the nearby emissions (hence with larger DFS values). However, focusing only on central Paris makes the E network less efficient for controlling the emissions in the rural area (see the spatial distribution of the energy, building and road emissions in Fig. 4a–c). This is because there are large point sources (e.g. the EDF Porcheville power plant and the TOTAL Grandpuits refinery from the energy sector; Fig. 2) and considerable building emissions located outside of the largest ring of the E networks (Figs. 3 and 4). The more extended U networks perform better than the smaller U networks and the equal-sized E networks in clarifying the negative cross correlations in errors of emission estimates for different sectors (see Fig. 9b–d for cross correlations between building, road, and energy sectors). The enhanced negative correlations would lead to decreased uncertainties in the total emission estimate that is the sum of sectoral emission estimates. This is a result that can also be found in finance where diversification in assets (weak and negative correlations between assets) reduces the portfolio risk (uncertainty in total assets). Notably, the E networks perform better than the U networks for estimating emissions from the airline sector. This is due to the fact that airport emissions (see Figs. 2 and 4f) are located between the two outer rings of the E networks. Moreover, the E networks per-

**Atmospheric inversion for cost effective quantification of city CO<sub>2</sub> emissions**

L. Wu et al.

Title Page

Abstract

Introduction

Conclusions

References

Tables

Figures



Back

Close

Full Screen / Esc

Printer-friendly Version

Interactive Discussion







theless our inversions were based on the experience from Bréon et al. (2015) in which real data from a few number of stations around Paris were used.

Two strategies may improve the performance of atmospheric inversion for MRV use at the city scale when using real data. First, the inversion framework can incorporate much richer sets of atmospheric observations. Recently, city networks have become increasingly densified, embracing other types of CO<sub>2</sub> measuring platforms such as eddy-covariance flux towers (Nordbo et al., 2012; Velasco et al., 2014), ground-based remote sensing instrument (Gisi et al., 2012), aircraft and satellites (Kort et al., 2012; Silva et al., 2013; Buchwitz et al., 2013). The benefit from assimilating these measurements however needs to be assessed. For instance, the inversion may suffer from limited representativeness of observations in space (e.g. 0.2–5 km<sup>2</sup> for eddy-covariance flux measurements; Christen, 2014) or in time (e.g. aircraft campaigns being relatively short due to their cost), or from a weak sensitivity of the observations to emissions (e.g. satellite column measurements). In contrast, some atmospheric tracers other than CO<sub>2</sub> can carry distinct signatures from different sectors, thereby their assimilation will certainly improve the ability of inversions to separate emissions from major sectors. For instance, radiocarbon (<sup>14</sup>C) measurements can serve for separating anthropogenic (fossil fuel combustion) and biogenic (biofuel and human and plant respiration) sources, and stable carbon isotope measurements (<sup>13</sup>C) can further distinguish combustions from gas or liquid fuel (Lopez et al., 2013; Vogel et al., 2013). CO, NO<sub>x</sub> and other co-emitted gases can be used as proxies for the estimation of sectoral CO<sub>2</sub> emissions (Vogel et al., 2010; Lopez et al., 2013; Turnbull et al., 2015). For example, NO<sub>x</sub> has a short life time. Therefore it is an appropriate tracer of local road transport emissions. The ratios between CO and fossil fuel CO<sub>2</sub> vary as a function of the local emission scenarios e.g. residential heating, road transport and industrial combustions, but note that this variation is ambiguous (Ammoura et al., 2014).

Second, further designs of the inversion system may be beneficial for improving the performance of the inversion. For instance, the procedure for selecting upwind stations can be refined by introducing time lags between downwind and upwind observations

**Atmospheric  
inversion for cost  
effective  
quantification of city  
CO<sub>2</sub> emissions**

L. Wu et al.

Title Page

Abstract

Introduction

Conclusions

References

Tables

Figures

◀

▶

◀

▶

Back

Close

Full Screen / Esc

Printer-friendly Version

Interactive Discussion



## Atmospheric inversion for cost effective quantification of city CO<sub>2</sub> emissions

L. Wu et al.

Title Page

Abstract

Introduction

Conclusions

References

Tables

Figures

◀

▶

◀

▶

Back

Close

Full Screen / Esc

Printer-friendly Version

Interactive Discussion

that are computed taking into account the wind directions and magnitudes precisely. We have shown in this study that the inversions are sensitive to the network type. This motivates optimal network design studies, which can be performed by some empirical rules (e.g. redistributing more stations along road network or around power plants to better distinguish emissions from road transport and energy production). Advanced network design topics include optimization algorithms that select optimal locations for the redistribution of stations (Wu and Bocquet, 2011) and tracking algorithms that select optimal locations for mobile stations (Abida and Bocquet, 2009). Given a fixed network, the sensitivity of concentration gradients to emissions may be increased by designing an adaptive spatiotemporal resolution of the emissions to which the scaling factors apply (Wu et al., 2011). When both the network and the resolution of emissions are fixed, the errors in the observations and in the prior emissions can be estimated for more credible inversions (Wu et al., 2013).

Further developing the current city scale inventories is a natural choice for emission accounting, following the applications of national inventories under UNFCCC and the Kyoto Protocol. Such refinement requires tedious efforts in order to continuously collect detailed and high-quality local data. In this paper, we demonstrated that atmospheric inversion could in principle achieve the same level of quality desired for estimates of total emissions at the same cost level.

Atmospheric inversion distinguishes itself in a number of ways for the quantification of city CO<sub>2</sub> emissions. First and foremost, it would provide an estimate using another method than inventories based on IPCC guidelines. Estimating the same source of emissions with two different approaches remains the best way to detect biases, even when the approaches may not be fully independent. Second, in addition to the verification of inventories, atmospheric inversion can also incorporate, whenever available, better inventories into its modeling framework to produce better emission estimates. Third, the inverse modeling system assimilating a cohort of measurements can provide a unique platform to investigate the urban carbon cycle (e.g. the anthropogenic/biogenic land–atmosphere carbon exchange of the urban ecosystem, and the



## Atmospheric inversion for cost effective quantification of city CO<sub>2</sub> emissions

L. Wu et al.

Title Page

Abstract

Introduction

Conclusions

References

Tables

Figures

◀

▶

◀

▶

Back

Close

Full Screen / Esc

Printer-friendly Version

Interactive Discussion

works. They only report at the annual and community resolution (Bertoldi et al., 2010; Cochran, 2015). Many of them adopt the 2006 IPCC Guidelines with adjustments to specific city context (City of Rio de Janeiro, 2011; Dienst et al., 2013) but without uncertainty quantification (Bellassen and Stephan, 2015); others follow the guidelines or methodologies developed by national/regional/local governments or non-profit local organizations/institutes (e.g. the Bilan Carbone methods in France; ADEME, 2010), as well as by international organizations – such as the newly proposed GPC standard designed by C40, Local Governments for Sustainability (ICLEI) and World Resources Institute (WRI) in the support of the World Bank, UN-HABITAT and UNEP. This type of inventories can cover indirect or embodied emissions that are linked with cities activities but occur outside the considered territories [the Scope 2 emissions related to the consumption of purchased electricity, heat or steam; and the Scope 3 emissions related to the consumption of other products and services not covered in Scope 2; see WRI/WBCSD (2011)]. In practice, the compilation of type-1 inventories can be performed with a limited cost that scales with the size of cities (e.g.  $\sim 18$  kEUR year<sup>-1</sup> for  $\sim 1$  million inhabitants excluding Scope 3 emissions; Cochran, 2015). To date, the type-1 inventories bear high and more importantly *undocumented* uncertainties.

The type 2 inventories are those that can be derived from global or regional gridded maps of emissions estimates which have been mainly used by the scientific community to model the atmospheric transport of CO<sub>2</sub>. Examples are the Emissions Database for Global Atmospheric Research (EDGAR) from the European Commission Joint Research Centre (JRC) and the Netherlands Environmental Assessment Agency (<http://edgar.jrc.ec.europa.eu>), the global/regional inventory developed by the Institute of Energy Economics and the Rational Use of Energy (IER) at the University of Stuttgart (Pregger et al., 2007), and the global fossil fuel CO<sub>2</sub> emission map from the Peking University (PKU-CO<sub>2</sub>; Wang et al., 2013). The activity data and emission factors entering in the fabrication of type-2 inventories are usually defined from scales coarser than the city scale, which leads to large and, again, *undocumented* uncertainty

locally. The type-2 inventories are free of charge for research purpose, and the fee for commercial use is insignificant.

The type 3 inventories are compiled based upon local data down to the building/street scale at the urban landscape. They are arguably more realistic than the two previous ones, but available for a small number of cities to our knowledge. Examples of this type are the AIRPARIF inventory for IDF (AIRPARIF, 2013), the London Atmospheric Emissions Inventory (LAEI; GLA, 2012), and the inventory from the HESTIA project for Indianapolis (Gurney et al., 2012). Developing a type-3 inventory is time consuming: it usually demands institutional efforts and requires a high level of expertise. Type-3 inventories can only be established in cities where good activity and/or fuel consumption data are accessible. The inventory quality would be better, if some central authority is responsible for ensuring that adequate data are consistently, transparently and timely reported by public and private players responsible for emissions. Uncertainty quantification for a type-3 inventory, being a difficult issue due to their complexity, nevertheless can be performed in an approximate way according to the expert judgment of the inventory compilers. As an example, the monthly uncertainty in the Paris type-3 inventory is estimated to be of the order of 20 % by the AIRPARIF engineers (see Bréon et al., 2015). The cost of type-3 inventories consists of data collection fee, salaries, and operation cost, and in general can be considered as at least one order of magnitude less than the notional cost target: 0.5 M EUR year<sup>-1</sup>.

Both type 2 and 3 inventories mainly account for direct emissions generated within the considered territories, which are the Scope 1 emissions. Scope 2 emissions for cities can be obtained from Scope 1 emissions. For instance, redistributing national/regional power plant emissions from type-2 inventories to urban areas can approximate a Scope 2 analysis (Marcotullio et al., 2013). Taking into account the energy produced outside of cities but consumed by cities will complete type-3 inventories to provide Scope 3 city emissions as well (AIRPARIF, 2013).

Whether belong to type-1, type-2 or type-3, the inventories at city scale are not frequently updated because the necessary data are usually disclosed and processed long

**Atmospheric  
inversion for cost  
effective  
quantification of city  
CO<sub>2</sub> emissions**

L. Wu et al.

Title Page

Abstract

Introduction

Conclusions

References

Tables

Figures

◀

▶

◀

▶

Back

Close

Full Screen / Esc

Printer-friendly Version

Interactive Discussion



## Atmospheric inversion for cost effective quantification of city CO<sub>2</sub> emissions

L. Wu et al.

Title Page

Abstract

Introduction

Conclusions

References

Tables

Figures



Back

Close

Full Screen / Esc

Printer-friendly Version

Interactive Discussion



after emissions actually happened. In case of revisions in calculation methods, such as the correction of emission factors or the addition of emitting activities that were ignored in the previous versions, the entire emission inventory has to be recomputed, which imposes a traceability framework for comparing different versions. In the case of the Paris type-3 inventory, there is only a new update every 2 years with a 2-years lag between the date of release and the corresponding year of emissions.

The IER inventory used in this OSSE study incorporates local data to provide a gridded inventory at 1 km and 1 h resolution. We detail this inventory in the main text of the paper (Sect. 3.4.1). Here we group the 40 sectors from this IER inventory into seven aggregate larger sectors, and list their annual budgets in Table A1.

### Appendix B: Network cost and instrumental details

We detail the network cost in Table B1, in which both expensive high precision sensors and cheaper sensors with limited, but acceptable precision are listed. The network cost includes not only the price of the sensors, but also other supplement items of equipment, network installation, maintenance, quality assurance and data processing. The estimated sensor cost is based on commercial available and prototype sensors being tested at the Laboratory of Climate and Environmental Sciences (LSCE). The cost of calibration is estimated to be of the same order for high precision and cheap sensors. The calibration for cheap sensors can be more frequent (e.g. two days) than for high precision sensors (e.g. one week), but needs less samples of calibration gas. In addition, innovative calibration procedures for cheap sensors are possible for further reductions of the calibration cost and the temporal correlation in instrument bias. For instance, a calibration center can be set up using high precision sensors to calibrate cheap sensors. One can manage two sets of cheap sensors: one in the calibration center and the other in situ in measuring. The calibration is simply performed by replacing the measuring sensors with recently calibrated ones from the calibration center. Since this new calibration method is free of calibration gas, and since the cost of replacing

sensors is very limited, one can maintain a high frequency of calibration (e.g. daily). Note that the network cost can, furthermore, be reduced when pre-existing infrastructure is available, for instance the installation could be free of cost if sharing with existing air quality monitoring platforms.

5 The total number of deployable monitoring sites is limited by the cost of the network. Given an budget limit of  $\sim 0.5$  M EUR year<sup>-1</sup>, one can include either  $\sim 10$  high precision sensors when starting from nothing or  $\sim 70$  low cost sensors with minimal installation and maintenance costs (Fig. B1). The local inventories may impose some case-specific additional cost (data fees or funding for a project), but this additional cost is at most an  
10 order of magnitude lower than the budget of  $\sim 0.5$  M EUR year<sup>-1</sup>.

### Appendix C: Trend detection under different levels of uncertainties in annual emission estimates

Supposing that the annual fossil fuel emissions from the Paris metropolitan area have a linear trend with a 25 % reduction in 15 years, and that the annual emission estimates  
15 have an 5 or 10 % uncertainty, we perform Monte Carlo simulations to check to what extent that the linear trend can be detected from perturbed annual emission estimates (within the given annual uncertainty) along years. The detection results are shown in Fig. C1. With 5 % annual emission uncertainty, the 25 % reduction of emissions in a 15-year horizon can be detected within [18, 32 %] at 95 % confidence level. In  
20 contrast, with 10 % annual emission uncertainty, the corresponding detection interval is [11, 39 %] at 95 % confidence level.

**The Supplement related to this article is available online at  
doi:10.5194/acpd-15-30693-2015-supplement.**

25 *Acknowledgements.* This study is a contribution to the project MRV Sector funded by the European Climate Knowledge and Innovation Community (Climate-KIC). Four authors (L. Wu, G. Broquet, F. Vogel and P. Ciais) work with the industrial chair BridGES supported by the



**Atmospheric  
inversion for cost  
effective  
quantification of city  
CO<sub>2</sub> emissions**

L. Wu et al.

Title Page

Abstract

Introduction

Conclusions

References

Tables

Figures

◀

▶

◀

▶

Back

Close

Full Screen / Esc

Printer-friendly Version

Interactive Discussion



Boden, T. A., Marland, G., and Andres, R. J.: Global, Regional, and National Fossil-Fuel CO<sub>2</sub> Emissions, Carbon Dioxide Information Analysis Center, Oak Ridge National Laboratory, US Department of Energy, Oak Ridge, Tenn., USA, 2013.

Bousquet, P., Peylin, P., Ciais, P., Le Quéré, C., Friedlingstein, P., and Tans, P. P.: Regional changes in carbon dioxide fluxes of land and oceans since 1980, *Science*, 290, 1342–1346, doi:10.1126/science.290.5495.1342, 2000.

Boussetta, S., Balsamo, G., Beljaars, A., Panareda, A.-A., Calvet, J.-C., Jacobs, C., van den Hurk, B., Viterbo, P., Lafont, S., Dutra, E., Jarlan, L., Balzarolo, M., Papale, D., and van der Werf, G.: Natural land carbon dioxide exchanges in the ECMWF integrated forecasting system: implementation and offline validation, *J. Geophys. Res.*, 118, 5923–5946, doi:10.1002/jgrd.50488, 2013.

Bréon, F. M., Broquet, G., Puygrenier, V., Chevallier, F., Xueref-Remy, I., Ramonet, M., Dieudonné, E., Lopez, M., Schmidt, M., Perrussel, O., and Ciais, P.: An attempt at estimating Paris area CO<sub>2</sub> emissions from atmospheric concentration measurements, *Atmos. Chem. Phys.*, 15, 1707–1724, doi:10.5194/acp-15-1707-2015, 2015.

Broquet, G., Chevallier, F., Bréon, F.-M., Kadygrov, N., Alemanno, M., Apadula, F., Hammer, S., Haszpra, L., Meinhardt, F., Morguí, J. A., Necki, J., Piacentino, S., Ramonet, M., Schmidt, M., Thompson, R. L., Vermeulen, A. T., Yver, C., and Ciais, P.: Regional inversion of CO<sub>2</sub> ecosystem fluxes from atmospheric measurements: reliability of the uncertainty estimates, *Atmos. Chem. Phys.*, 13, 9039–9056, doi:10.5194/acp-13-9039-2013, 2013.

Buchwitz, M., Reuter, M., Bovensmann, H., Pillai, D., Heymann, J., Schneising, O., Rozanov, V., Krings, T., Burrows, J. P., Boesch, H., Gerbig, C., Meijer, Y., and Löscher, A.: Carbon Monitoring Satellite (CarbonSat): assessment of atmospheric CO<sub>2</sub> and CH<sub>4</sub> retrieval errors by error parameterization, *Atmos. Meas. Tech.*, 6, 3477–3500, doi:10.5194/amt-6-3477-2013, 2013.

Chang, J.-P. and Bellassen, V.: Trend setter for territorial schemes: national greenhouse gas inventories under the UNFCCC, in: *Accounting for Carbon: Monitoring, Reporting and Verifying Emissions in the Climate Economy*, edited by: Bellassen, V. and Stephan, N., Cambridge University Press, Cambridge, UK, 2015.

Chevallier, F., Ciais, P., Conway, T. J., Aalto, T., Anderson, B. E., Bousquet, P., Brunke, E. G., Ciattaglia, L., Esaki, Y., Fröhlich, M., Gomez, A., Gomez-Pelaez, A. J., Haszpra, L., Krummel, P. B., Langenfelds, R. L., Leuenberger, M., Machida, T., Maignan, F., Matsueda, H., Morguí, J. A., Mukai, H., Nakazawa, T., Peylin, P., Ramonet, M., Rivier, L., Sawa, Y., Schmidt, M., Steele, L. P., Vay, S. A., Vermeulen, A. T., Wofsy, S., and Worthy, D.: CO<sub>2</sub>





## Atmospheric inversion for cost effective quantification of city CO<sub>2</sub> emissions

L. Wu et al.

Title Page

Abstract

Introduction

Conclusions

References

Tables

Figures

◀

▶

◀

▶

Back

Close

Full Screen / Esc

Printer-friendly Version

Interactive Discussion

IGES: Measurement, Reporting and Verification (MRV) for Low Carbon Development: Learning from Experience in Asia, IGES Policy Report No. 2012-03, Institute for Global Environmental Strategies (IGES), Kanagawa, Japan, 2012.

Kort, E. A., Frankenberg, C., Miller, C. E., and Oda, T.: Space-based observations of megacity carbon dioxide, *Geophys. Res. Lett.*, 39, L17806, doi:10.1029/2012gl052738, 2012.

Kort, E. A., Angevine, W. M., Duren, R., and Miller, C. E.: Surface observations for monitoring urban fossil fuel CO<sub>2</sub> emissions: minimum site location requirements for the Los Angeles megacity, *J. Geophys. Res.*, 118, 1577–1584, doi:10.1002/jgrd.50135, 2013.

Latoska, A.: Erstellung eines räumlich hoch aufgelösten Emissionsinventar von Luftschadstoffen am Beispiel von Erstellung eines räumlich hoch aufgelösten, Thesis, Institut für Energiewirtschaft und Rationelle Energieanwendung, Universität Stuttgart, 2009.

Lauvaux, T., Miles, N. L., Richardson, S. J., Deng, A., Stauffer, D. R., Davis, K. J., Jacobson, G., Rella, C., Calonder, G.-P., and DeCola, P. L.: Urban emissions of CO<sub>2</sub> from Davos, Switzerland: the first real-time monitoring system using an atmospheric inversion technique, *J. Appl. Meteorol. Clim.*, 52, 2654–2668, doi:10.1175/jamc-d-13-038.1, 2013.

Liu, Z., He, C., Zhou, Y., and Wu, J.: How much of the world's land has been urbanized, really? A hierarchical framework for avoiding confusion, *Landscape Ecol.*, 29, 763–771, doi:10.1007/s10980-014-0034-y, 2014.

Lopez, M., Schmidt, M., Delmotte, M., Colomb, A., Gros, V., Janssen, C., Lehman, S. J., Mondelain, D., Perrussel, O., Ramonet, M., Xueref-Remy, I., and Bousquet, P.: CO, NO<sub>x</sub> and <sup>13</sup>CO<sub>2</sub> as tracers for fossil fuel CO<sub>2</sub>: results from a pilot study in Paris during winter 2010, *Atmos. Chem. Phys.*, 13, 7343–7358, doi:10.5194/acp-13-7343-2013, 2013.

Mairie de Paris: BLEU Climat 2012, l'engagement de la collectivité parisienne en matière de lutte contre les émissions de gas à effet de serre et d'efficacité énergétique, available at: <http://api-site-cdn.paris.fr/images/110876.pdf> (last access: 2 November 2015), 2012.

Marcotullio, P., Sarzynski, A., Albrecht, J., Schulz, N., and Garcia, J.: The geography of global urban greenhouse gas emissions: an exploratory analysis, *Climatic Change*, 121, 621–634, doi:10.1007/s10584-013-0977-z, 2013.

Marr, M. A. and Wehner, S.: Cities and Carbon Finance: a Feasibility Study on an Urban CDM, UNEP (United Nations Environment Programme)/Gwangju City, 2012.

McKain, K., Wofsy, S. C., Nehrkorn, T., Eluszkiewicz, J., Ehleringer, J. R., and Stephens, B. B.: Assessment of ground-based atmospheric observations for verification of greenhouse

## Atmospheric inversion for cost effective quantification of city CO<sub>2</sub> emissions

L. Wu et al.

Title Page

Abstract

Introduction

Conclusions

References

Tables

Figures

◀

▶

◀

▶

Back

Close

Full Screen / Esc

Printer-friendly Version

Interactive Discussion

gas emissions from an urban region, P. Natl. Acad. Sci. USA, 109, 8423–8428, doi:10.1073/pnas.1116645109, 2012.

Meinshausen, M., Meinshausen, N., Hare, W., Raper, S. C. B., Frieler, K., Knutti, R., Frame, D. J., and Allen, M. R.: Greenhouse-gas emission targets for limiting global warming to 2 °C, Nature, 458, 1158–1162, 2009.

Menut, L., Bessagnet, B., Khvorostyanov, D., Beekmann, M., Blond, N., Colette, A., Coll, I., Curci, G., Foret, G., Hodzic, A., Mailler, S., Meleux, F., Monge, J.-L., Pison, I., Siour, G., Turquety, S., Valari, M., Vautard, R., and Vivanco, M. G.: CHIMERE 2013: a model for regional atmospheric composition modelling, Geosci. Model Dev., 6, 981–1028, doi:10.5194/gmd-6-981-2013, 2013.

Ninomiya, Y.: Classification of MRV of Greenhouse Gas (GHG) Emissions/Reductions: for the Discussions on NAMAs and MRV, Institute for Global Environmental Strategies (IGES), Policy Brief, Number 25, 2012.

Nordbo, A., Järvi, L., Haapanala, S., Wood, C. R., and Vesala, T.: Fraction of natural area as main predictor of net CO<sub>2</sub> emissions from cities, Geophys. Res. Lett., 39, L20802, doi:10.1029/2012gl053087, 2012.

Pacala, S., Breidenich, C., Brewer, P. G., Fung, I., Gunson, M. R., Heddle, G., Law, B., Marland, G., Paustian, K., and Prather, K.: Verifying Greenhouse Gas Emissions: Methods to Support International Climate Agreements, The National Academies Press, Washington, DC, 124 pp., 2010.

Peters, W., Jacobson, A. R., Sweeney, C., Andrews, A. E., Conway, T. J., Masarie, K., Miller, J. B., Bruhwiler, L. M. P., Pétron, G., Hirsch, A. I., Worthy, D. E. J., van der Werf, G. R., Randerson, J. T., Wennberg, P. O., Krol, M. C., and Tans, P. P.: An atmospheric perspective on North American carbon dioxide exchange: CarbonTracker, P. Natl. Acad. Sci. USA, 104, 18925–18930, doi:10.1073/pnas.0708986104, 2007.

PLF: État récapitulatif de l'effort financier consenti en 2014 et prévu en 2015 au titre de la protection de la nature et de l'environnement, Projet de loi de finances (PLF) pour 2015 – Jaunes budgétaires, Ministère français des finances et des comptes publics, available at: [http://www.performance-publique.budget.gouv.fr/sites/performance\\_publicque/files/farandole/ressources/2015/pap/pdf/jaunes/jaune2015\\_environnement.pdf](http://www.performance-publique.budget.gouv.fr/sites/performance_publicque/files/farandole/ressources/2015/pap/pdf/jaunes/jaune2015_environnement.pdf) (last access: 2 November 2015), 2014

Pregger, T., Scholz, Y., and Friedrich, R.: Documentation of the Anthropogenic GHG Emission Data for Europe Provided in the Frame of CarboEurope GHG and CarboEurope IP, Final







## Atmospheric inversion for cost effective quantification of city CO<sub>2</sub> emissions

L. Wu et al.

Title Page

Abstract

Introduction

Conclusions

References

Tables

Figures

◀

▶

◀

▶

Back

Close

Full Screen / Esc

Printer-friendly Version

Interactive Discussion

**Table 1.** Spatiotemporal resolutions of the sectoral control factors for inversions over 30-day periods (see the main text and Table A1 for more information on aggregate sectors).

Control factors	Spatial resolution	Time resolution	Number of factors
Building	5 zone	Daily daytime and night-time	300
Road	5 zones	Daily daytime and night-time	300
Energy	1 zone	Daily daytime and night-time	60
Production	1 zone	Daily daytime and night-time	60
Agriculture	1 zone	Daily	30
Airline	1 zone	Daily	30
Rest	1 zone	Daily	30
NEE	1 zone	5-day period with four daily 6 h-windows	24
–	–	–	834 (total)

**Table A1.** Specification of all the 40 sectors in the IER inventory employed in this study. These sectors are grouped into seven aggregate larger sectors listed in Table 1.

Sector	NFR code	Budget (TgCyr <sup>-1</sup> )	Comments
Energy	1A1a	3.7205	Public Electricity and Heat Production
	1A1b	0.31007	Petroleum Refining
	1A1c	0.097906	Manufacture of Solid Fuels and Other Energy Industries
Road	1A3bi	3.0287	Passenger cars
	1A3biii	0.78072	Heavy duty vehicles
	1A3bii	0.66808	Light duty vehicles
Building	1A4bi	2.5757	Residential plants
	1A4ai	1.0185	Commercial/Institutional
	1A4bii	0.90577	Household and gardening (mobile)
	1A4aii	0.4489	Commercial/Institutional
Production	1A2fi	1.0724	Fuel Combustion Activities: manufacturing Industries and Construction
	1A2c	0.37312	Chemicals
	2A1	0.11867	Mineral Products
	1A2e	0.11245	Food Processing, Beverages & Tobacco
	1A2a	0.09999	Iron and Steel
	1A2d	0.088409	Pulp, Paper and Print
Agriculture	1A4ci	0.32116	Plants in agriculture, forestry and aquaculture
	1A4cii	0.14497	Off-road Vehicles and Other Machinery
Airline	1A3ai(i)	0.58194	International Aviation
	1A3aii(i)	0.34983	Civil Aviation (Domestic)
Rest	2B1	0.075718	Ammonia Production
	6Cb	0.042929	Waste Incineration
	3A2	0.038744	Paint Application
	1A3biv	0.037411	Automobile tyre and brake wear
	1A3e	0.031093	Other Transportation
	2C1	0.020038	Metal Production
	1A3c	0.019035	Railways
	2A7d	0.011561	Mineral Products
	2A4	0.0082194	Mineral Products
	2B5a	0.0075701	Chemical Industry
	3C	0.0056263	Chemical Products, Manufacture and Processing
	2A3	0.0054513	Mineral Products
	1A2b	0.00506	Non-ferrous Metals
	2A2	0.0049208	Mineral Products
	2C3	0.0044444	Metal Production
	1A3dii	0.0039965	Navigation
	2C2	0.0024742	Metal Production
3B1	0.0017747	Degreasing and Dry Cleaning	
1B1b	0.00018562	Fugitive Emissions from Fuels	
2B3	0.00013253	Chemical Industry	

**Atmospheric inversion for cost effective quantification of city CO<sub>2</sub> emissions**

L. Wu et al.

Title Page

Abstract Introduction

Conclusions References

Tables Figures

◀ ▶

◀ ▶

Back Close

Full Screen / Esc

Printer-friendly Version

Interactive Discussion





**Atmospheric inversion for cost effective quantification of city CO<sub>2</sub> emissions**

L. Wu et al.

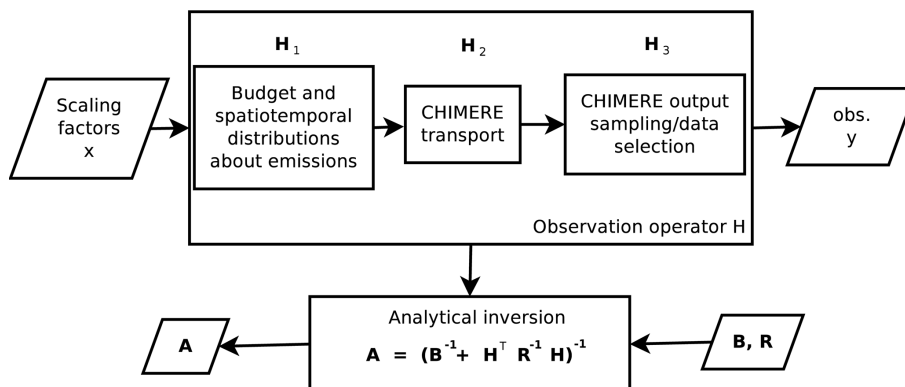


**Figure 1.** Diagram of the synthetic study on atmospheric inversion of city CO<sub>2</sub> emissions.

Title Page

Abstract Introduction

Conclusions References

Tables Figures

◀ ▶

◀ ▶

Back Close

Full Screen / Esc

Printer-friendly Version

Interactive Discussion



## Atmospheric inversion for cost effective quantification of city CO<sub>2</sub> emissions

L. Wu et al.

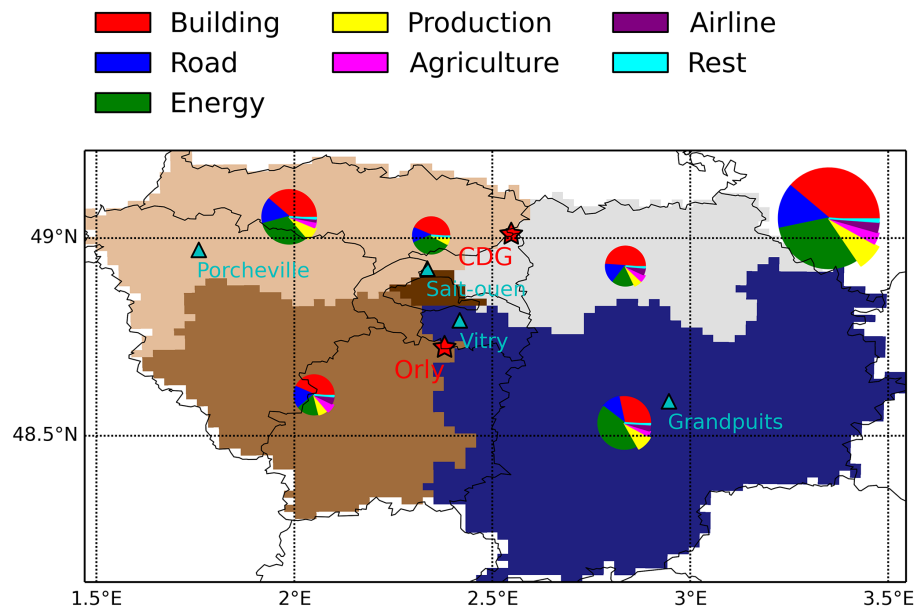


**Figure 2.** Sectoral budgets of fossil fuel CO<sub>2</sub> emissions from the IER inventory for five zones of IDF for the month of January in 2011 (see the first seven rows in Table 1 for sector specifications). The circle area is proportional to the emission budget. The upper right largest circle shows the total sectoral budgets for all the five zones of IDF. The red pentagons shows the two airports CDG and Orly, and the cyan triangles show several large point emissions such as three EDF power plants and the TOTAL Grandpuits refinery.

[Title Page](#)
[Abstract](#)
[Introduction](#)
[Conclusions](#)
[References](#)
[Tables](#)
[Figures](#)
[◀](#)
[▶](#)
[◀](#)
[▶](#)
[Back](#)
[Close](#)
[Full Screen / Esc](#)
[Printer-friendly Version](#)
[Interactive Discussion](#)

## Atmospheric inversion for cost effective quantification of city CO<sub>2</sub> emissions

L. Wu et al.

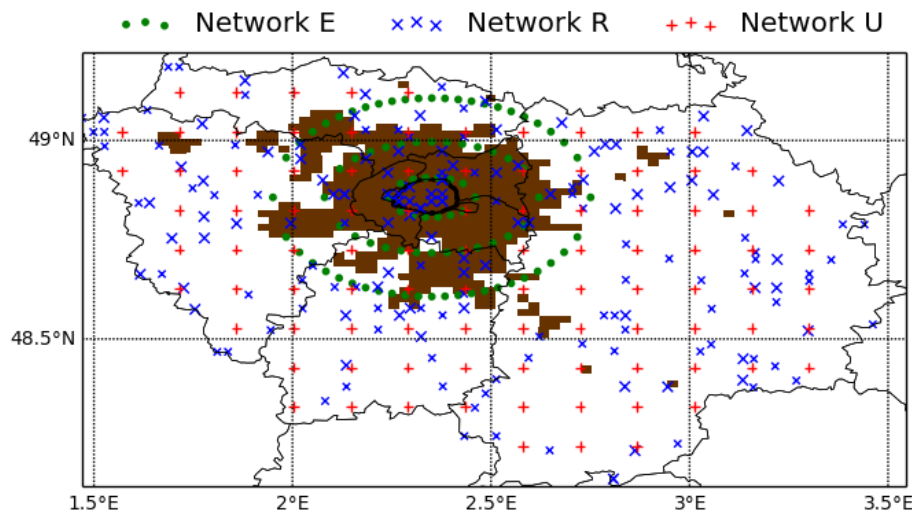


**Figure 3.** Illustrative locations for the elliptical (E), random-even (R) and unifrom (U) networks over IDF. The brown area marks out where the population density is larger than  $1250 \text{ people km}^{-2}$ . The E network marked by green dots consists of three rings surrounding the densely populated urban area in brown. The U network (red crosses) extends to the regular grid points of the IDF domain. The site locations of the R network are randomly selected respectively in three concentric areas: (1) the city center within the peripheral ring (coinciding with the smallest green ring), (2) the suburban area (in brown) with central Paris clipped out, and (3) the rest of IDF.

[Title Page](#)
[Abstract](#)
[Introduction](#)
[Conclusions](#)
[References](#)
[Tables](#)
[Figures](#)
[◀](#)
[▶](#)
[◀](#)
[▶](#)
[Back](#)
[Close](#)
[Full Screen / Esc](#)
[Printer-friendly Version](#)
[Interactive Discussion](#)

# Atmospheric inversion for cost effective quantification of city CO<sub>2</sub> emissions

L. Wu et al.

Title Page

Abstract

Introduction

Conclusions

References

Tables

Figures

◀

▶

◀

▶

Back

Close

Full Screen / Esc

Printer-friendly Version

Interactive Discussion

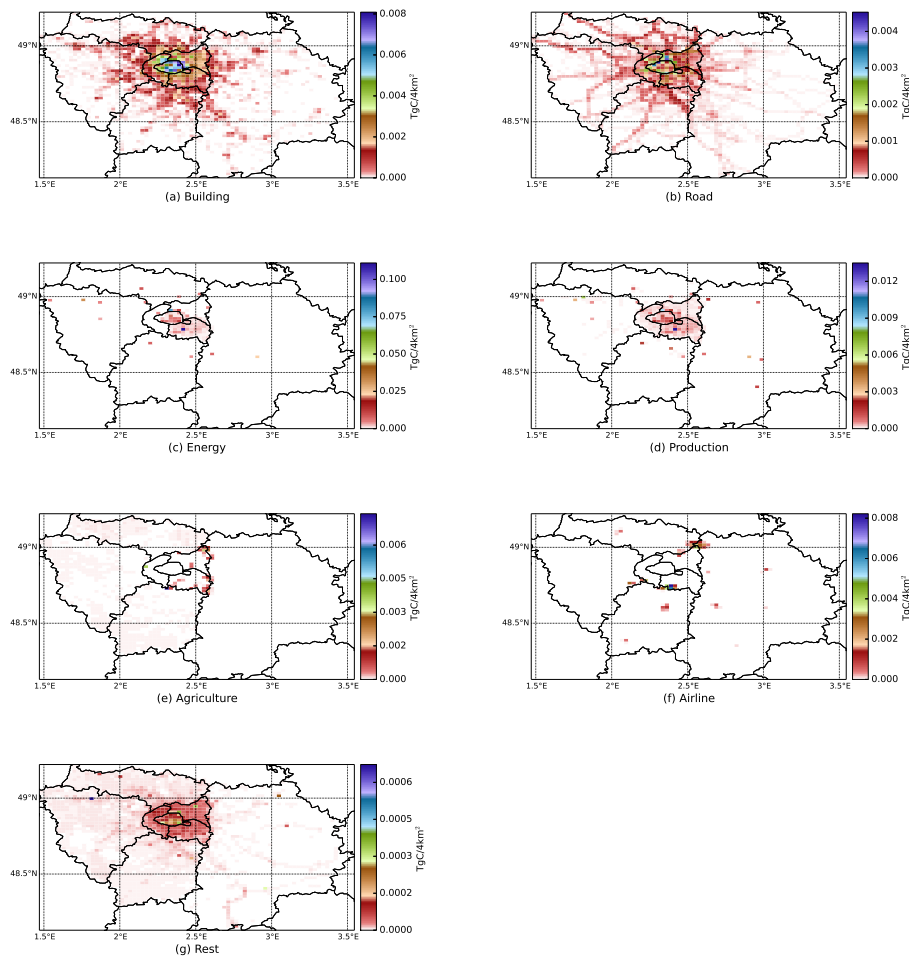


**Figure 4.** Sectoral and spatial distribution of the IER inventory for IDF for January 2011.

## Atmospheric inversion for cost effective quantification of city CO<sub>2</sub> emissions

L. Wu et al.

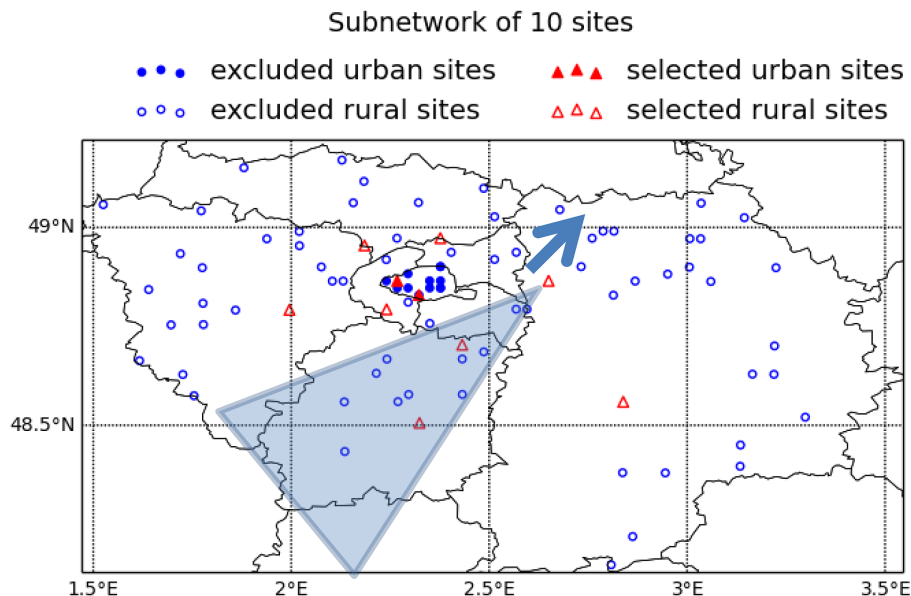


**Figure 5.** Selection a subset (10 sites marked out in red triangles) from a cloud of candidate locations for the R network to form smaller networks. The circles show the sites that are not selected. The open circles/triangles are for rural sites, and the filled circles/triangles are for urban sites. This figure also shows how the wind direction selects candidates of upwind sites for concentration gradient computations at a downwind station. The blue arrow indicates the wind direction at that downwind station. The two red triangles covered in the shadow area are candidate upwind sites according to the selection procedure detailed in the main text of this paper.

[Title Page](#)[Abstract](#)[Introduction](#)[Conclusions](#)[References](#)[Tables](#)[Figures](#)[◀](#)[▶](#)[◀](#)[▶](#)[Back](#)[Close](#)[Full Screen / Esc](#)[Printer-friendly Version](#)[Interactive Discussion](#)

## Atmospheric inversion for cost effective quantification of city CO<sub>2</sub> emissions

L. Wu et al.

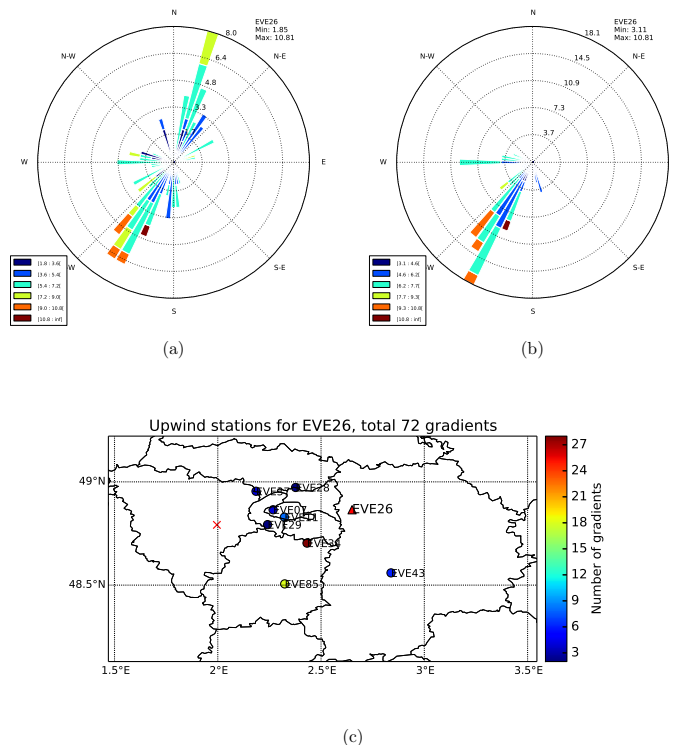


**Figure 6.** Results of selections of upwind stations for gradient computations for one downwind station for the month of January in 2011. Here we use a R network of 10 stations defined in Fig. 5. The illustrative downwind station in Fig. 5 (named EVE26 in this figure) is chosen for diagnosis. **(a)** The afternoon wind conditions at EVE26 during the given month; **(b)** the afternoon wind conditions for selected observations for gradient calculation at EVE26; **(c)** the counts of times selected as the upwind site for gradient computations at EVE26 for all the other nine stations. The leftmost red cross indicates that this site is never selected for gradient computation for EVE26.

## Atmospheric inversion for cost effective quantification of city CO<sub>2</sub> emissions

L. Wu et al.

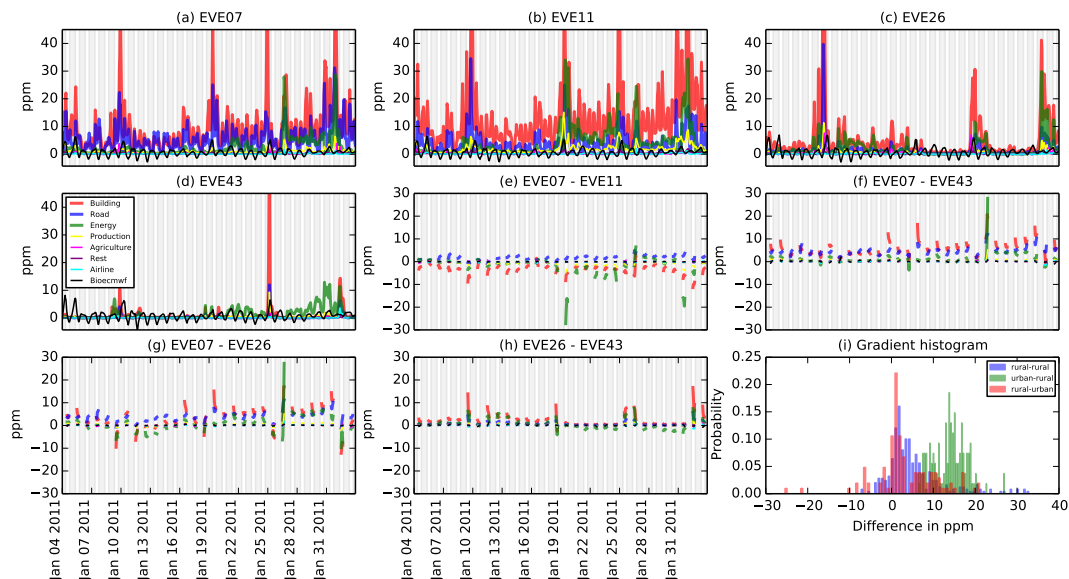
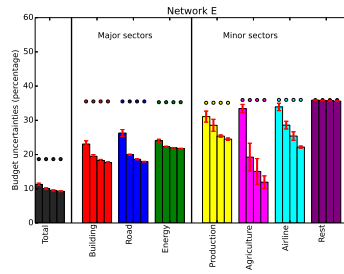


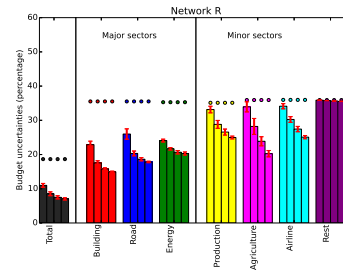
**Figure 7.** (a–d) CO<sub>2</sub> mixing ratio series of sectoral CHIMERE simulations at four selected stations of the R network (see Figs. 5 and 6c). EVE07 and EVE11 are urban sites and EVE26 and EVE43 are rural sites but close to large point emissions. The shadow marks out the night time. (e–h) The time series of the difference in model simulations sampled at several site pairs among the four sites. (i) The histogram of afternoon concentration gradients following the data selection procedure detailed in Sect. 3.4.3 for all the 10 stations of the R network. These histograms are grouped according to the type of downwind and upwind stations.

## Atmospheric inversion for cost effective quantification of city CO<sub>2</sub> emissions

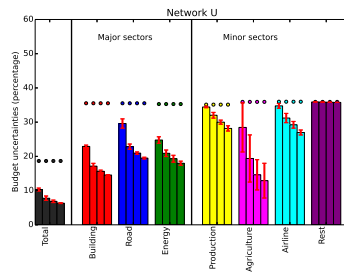
L. Wu et al.



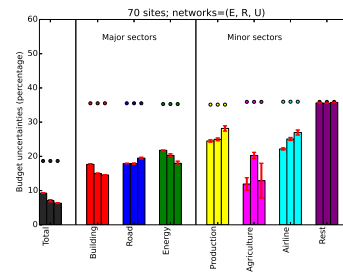
(a)



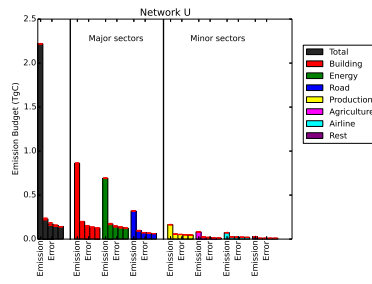
(b)



(c)



(d)



Title Page

Abstract

Introduction

Conclusions

References

Tables

Figures

◀

▶

◀

▶

Back

Close

Full Screen / Esc

Printer-friendly Version

Interactive Discussion



**Figure 8.** Budget of uncertainties in total and sectoral emission estimates by inversions using three types of networks of different sizes. Each sector has a distinct color. In **(a–d)**, we show the uncertainty budgets in percentage to the corresponding emission budgets computed using the IER inventory. The points indicate the percentage of prior uncertainty budgets before inversion, and the bars demonstrate the percentage of posterior uncertainty budgets after inversion. The error bars show the variations of the uncertainty budget using 10 different networks of same size (10, 30, 50, or 70) constructed as detailed in Sect. 3.3. **(a–c)** Reduction of uncertainties by inversions using three different types of networks of increasing sizes. For each sector, the numbers of stations corresponding to the four bars from left to right are 10, 30, 50 and 70 stations respectively. **(d)** Reduction of uncertainties by inversions using three different types of networks of 70 stations. The types of network corresponding to the three bars from left to right are E, R, and U respectively. **(e)** Comparison between the inventory budgets and uncertainty budgets (both in TgC) using the uniform network of increasing sizes. For each sector, the leftmost bar shows the inventory budget, and the four remaining bars to the right show the budget of uncertainties in posterior emission estimates by inversions using 10, 30, 50 and 70 stations respectively.

## Atmospheric inversion for cost effective quantification of city CO<sub>2</sub> emissions

L. Wu et al.

Title Page

Abstract

Introduction

Conclusions

References

Tables

Figures

◀

▶

◀

▶

Back

Close

Full Screen / Esc

Printer-friendly Version

Interactive Discussion

## Atmospheric inversion for cost effective quantification of city CO<sub>2</sub> emissions

L. Wu et al.

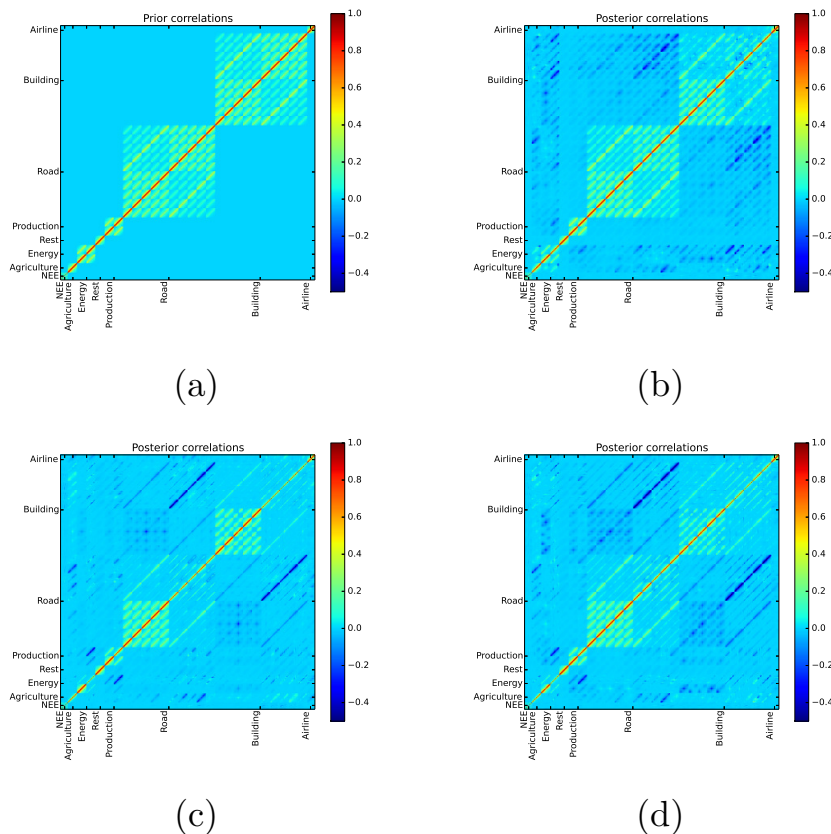


**Figure 9.** The correlation structures in **(a)** the error of prior scaling factor estimates; **(b)** the posterior error obtained by inversion using a U network with 10 stations; **(c)** the posterior error obtained by inversion using an E network with 70 stations; and **(d)** the posterior error obtained by inversion using a U network with 70 stations.

## Atmospheric inversion for cost effective quantification of city CO<sub>2</sub> emissions

L. Wu et al.

Title Page

Abstract

Introduction

Conclusions

References

Tables

Figures

◀

▶

◀

▶

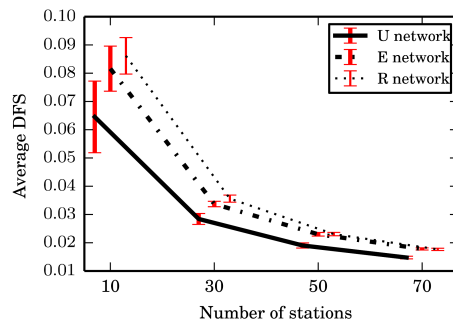
Back

Close

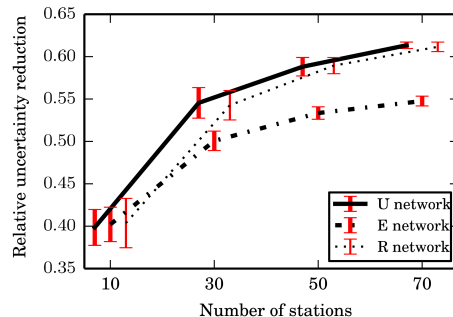
Full Screen / Esc

Printer-friendly Version

Interactive Discussion



(a)



(b)

**Figure 10.** For three types of networks of different sizes, we compute **(a)** the average number of Degrees of Freedom for the Signal (DFS/ $d$  where  $d$  is the total number of observations assimilated) accounting for, on average, the independent pieces of information from an observation to resolve emissions; and **(b)** the relative reduction of uncertainties in scaling factor estimates computed by  $(\sqrt{\mathbf{1}^T \mathbf{B} \mathbf{1}} - \sqrt{\mathbf{1}^T \mathbf{A} \mathbf{1}}) / \sqrt{\mathbf{1}^T \mathbf{B} \mathbf{1}}$ , where  $\mathbf{1}$  is an all-one vector. The error bars show variations due to inversions using 10 different networks of same size constructed as detailed in Sect. 3.3.

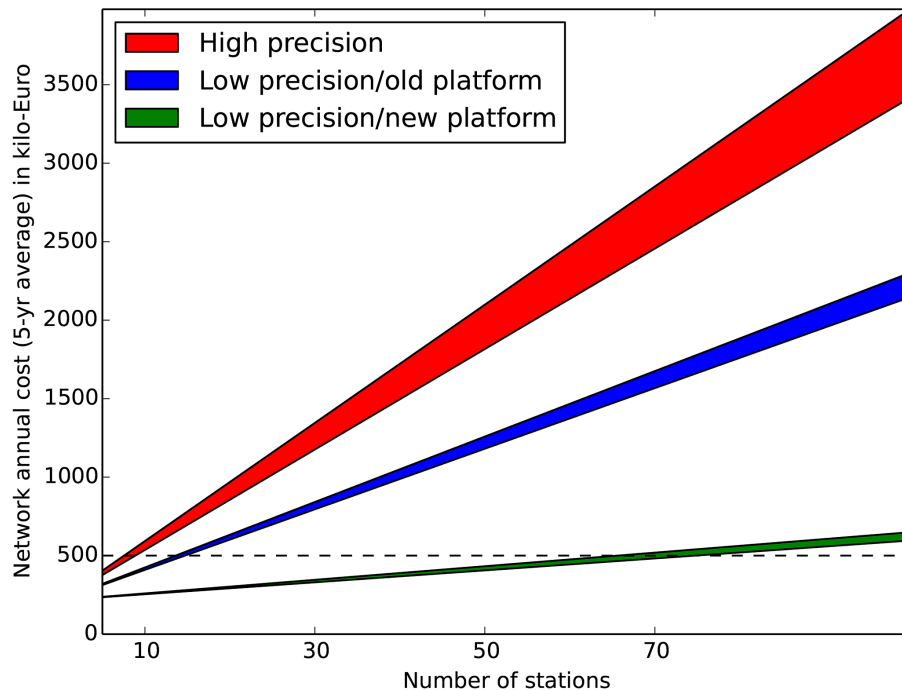


**Figure B1.** Sketch diagram on the cost of networks with either high precision sensors or low cost sensors as a function of increasing number of sites. For new platform, pre-existing infrastructure is used for saving cost. The range of cost corresponds to different levels of depreciation rate listed in Table B1.

**Atmospheric inversion for cost effective quantification of city CO<sub>2</sub> emissions**

L. Wu et al.

Title Page	
Abstract	Introduction
Conclusions	References
Tables	Figures
◀	▶
◀	▶
Back	Close
Full Screen / Esc	
Printer-friendly Version	
Interactive Discussion	



## Atmospheric inversion for cost effective quantification of city CO<sub>2</sub> emissions

L. Wu et al.

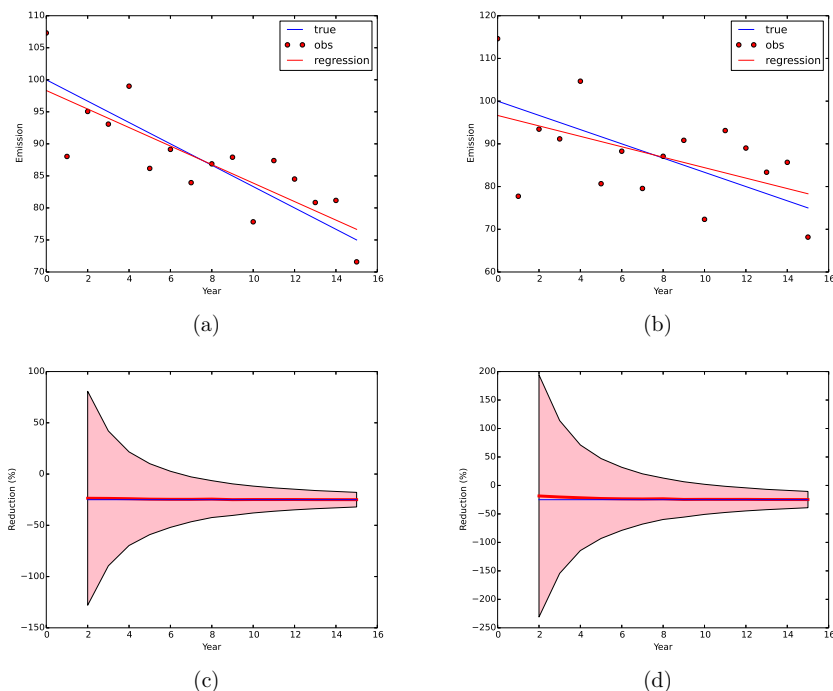


**Figure C1.** Detection of linear trends using the Monte Carlo method with ensembles of 10 000 simulations. We hypothesize that the emissions decrease linearly from a value of 100 in any appropriate unit to 75 (i.e. a 25 % reduction) in a 15-years time horizon. **(a and b)** show the linear trends detected by linear regressions (red lines) using series of emissions, which are obtained by perturbing the hypothesized emission values (blue lines) under 5 and 10 % 2-sigma annual emission uncertainties respectively (in percentage to the emission value in the initial year). **(c and d)** show the increasing 2-sigma accuracy of the trend detections with increasingly available emission data along years. The detection accuracy is calculated from statistics of regression results for 10 000 simulations.